

## Spatiotemporal Control of Migration of Single Cells on a Photoactivatable Cell Microarray

Jun Nakanishi,<sup>\*,†,‡,§,¶</sup> Yukiko Kikuchi,<sup>†,¶</sup> Satoshi Inoue,<sup>#</sup> Kazuo Yamaguchi,<sup>#</sup> Tohru Takarada,<sup>\*,†</sup> and Mizuo Maeda<sup>†</sup>

Bioengineering Laboratory, Discovery Research Institute, RIKEN, 2-1 Hirosawa, Wako, Saitama 351-0198, Japan, PRESTO, Japan Science and Technology Agency (JST), 4-1-8 Honcho, Kawaguchi, Saitama 332-0012, Japan, Institute for Biomedical Engineering, Consolidated Research Institute for Advanced Science and Medical Care, Waseda University, 513 Wasedaturumaki-cho, Shinjuku-ku Tokyo 162-0041, Japan, and Department of Materials Science, Faculty of Science, Kanagawa University, 2946 Tsuchiya, Hiratsuka, Kanagawa 259-1293, Japan

Received January 15, 2007; E-mail: nakanishi.jun@nims.go.jp; ttkrd@riken.go.jp

Cell migration is a fundamental biological activity involved in biological processes such as development, wound healing, and tumor metastasis.<sup>1</sup> Each cell experiences highly integrated multisteps to move itself forward.<sup>2</sup> To study the migrating behavior of individual cells, it is important to control migration of each single cell and analyze it microscopically. A number of methods have recently been developed, including methods based on electroactive self-assembled monolayers,<sup>3–5</sup> microelectrodes,<sup>6</sup> microfluidics,<sup>7–9</sup> and layer-by-layer polymeric materials.<sup>10</sup> However, these methods usually treat cells that have unavoidable variations in shape, orientation, or the number of contacting cells. Because cells under these environmental conditions often display a distribution of heterogeneous behaviors, creation of uniform environments for individual cells is important for investigating fundamental cellular processes in further detail.<sup>11</sup> Recently, a platform for analyzing the migration of single cells based on microcontact printing technology has been reported, whereby the relationship of cell migration and cellular geometries has been elucidated.<sup>12–14</sup>

Here, we present a photochemical method for spatiotemporal control of the migration of single cells. This method is based on our previous reports,<sup>15,16</sup> where we demonstrated cell patterning, co-culturing, and induction of migration of multiple cells using a functional substrate that changes from non-cell-adhesive to cell-adhesive by UV illumination under a standard fluorescence microscope. In the present study, we applied this photoactivatable substrate to simultaneous tracking of the initial step of cell migration in a single-cell microarray format, which allowed for quantitative analysis of extension rates of cell protrusion.

The substrate was prepared by surface modification of a glass coverslip with a silane coupling agent, 1-(2-nitrophenyl)ethyl-11-trichlorosilylundecanoate, which develops a carboxyl group upon photochemical reaction (Figure 1a). The substrate was at first coated with tri-block copolymer Pluronic F108 to make the surface non-cell-adhesive.<sup>17</sup> The change in cell adhesiveness of this substrate was based on the photochemical reaction-driven surface hydrophilization, resulting in substitution of fibronectin, a cell-adhesive protein, for the Pluronic that had been adsorbed to the surface via hydrophobic interaction (Figure S1). Cell migration was induced by photoactivating a region alongside each single cell, which had been arrayed in advance on the substrate (Figure 1b).

In this study, migration of fibroblast-like NIH3T3 cells was examined as an example. This cell type stochastically extends broad

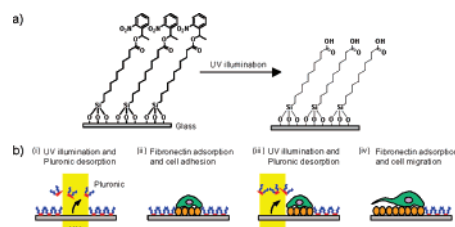


**Figure 1.** Spatiotemporal control of cell migration on the photoactivatable cell-culturing substrate. (a) The photochemical reaction on the substrate surface by UV illumination at 365 nm. (b) Schematic illustrations of the placement of single cells followed by the induction of cell migration on the substrate.

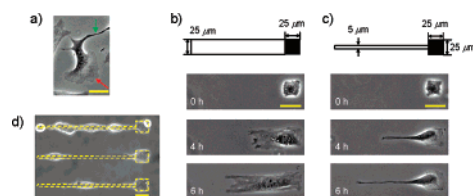


**Figure 2.** Selective induction of two characteristic protrusions in NIH3T3 cells. (a) Stochastic extension of protrusions led by a lamellipodium (red) and by a filopodium (green) on a fibronectin-coated nonpatterned surface. (b, c) Selective induction of protrusions by illuminating a wide path (b, 25  $\mu\text{m}$ ) or a narrow path (c, 5  $\mu\text{m}$ ) alongside the single cells. In upper figures, primary (black square) and secondary (white rectangle) illuminated regions are illustrated. Times after induction of cell migration are shown in the phase-contrast images. (d) Cell adhesion onto a substrate where square array spots and paths (5  $\mu\text{m}$ ) were illuminated simultaneously. Yellow dotted lines represent the illuminated region. All scale bars represent 25  $\mu\text{m}$ .

flat protrusions led by lamellipodia<sup>18</sup> and elongated thin protrusions led by filopodia<sup>19</sup> (Figure 2a). We arrayed single NIH3T3 cells on 25  $\times$  25  $\mu\text{m}^2$  square spots to keep individual cells separate with no variation in their shape and attaching area. Illumination of 25  $\mu\text{m}$  wide rectangular paths alongside the spots caused the cells to extend lamellipodia and to spread over the illuminated regions (Figure 2b). On the other hand, when 5  $\mu\text{m}$  wide paths alongside the spots were illuminated, the cells extended filopodia at their leading edges and formed thin protrusions along the illuminated paths (Figure 2c). Only a small portion of the tested cells (9%, 2 of 23) formed thin protrusions over the wide paths, a finding consistent with the fact that NIH3T3 cells extend filopodia stochastically on a nonpatterned surface (Figure 2a). In contrast, all of the tested cells (100%, 29 of 29) extended thin protrusions along the narrow paths. These results confirmed that selective induction of the two characteristic types of protrusions was realized by the present method. Successive photoactivation of the substrate after cell alignment (Figure 1b) is absolutely essential because cells

<sup>†</sup> RIKEN.

<sup>‡</sup> JST.

<sup>§</sup> Waseda University.

<sup>#</sup> Kanagawa University.

<sup>¶</sup> Current address: International Center for Young Scientists, National Institute for Materials Science, 1-1 Namiki, Tsukuba, Ibaraki 305-0044, Japan.

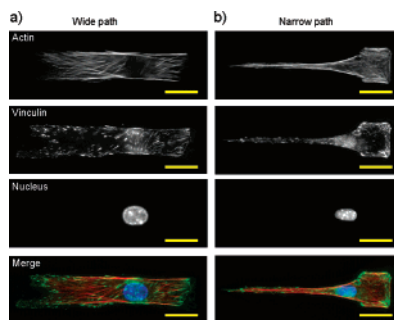


**Figure 3.** Actin cytoskeleton and subcellular structure of cells extending protrusions. NIH3T3 cells on the square spots were induced to extend cell protrusions by illuminating a wide path (a, 25  $\mu\text{m}$ ) and a narrow path (b, 5  $\mu\text{m}$ ). Cells were fixed at 6 h after induction of cell migration and were subjected to immunofluorescence staining. Actin, vinculin, and the nucleus were imaged in red, green, and blue, respectively. Scale bars (25  $\mu\text{m}$ ) are placed below the primary illuminated square spots.

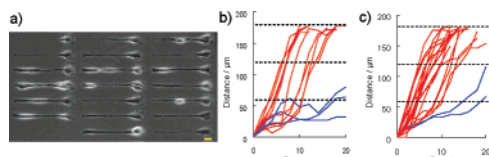


**Figure 4.** Quantitative analysis of cell migration in a single-cell microarray format. (a) A representative phase-contrast image of a single-cell microarray for the narrow path at 14 h after induction. Scale bar represents 25  $\mu\text{m}$ . (b, c) Time profiles of cell migration along the wide paths (b) and the narrow paths (c). The distance between the leading edge of the protrusion and the left edge of the primary square spot was plotted against time every 2 h after illumination. The leading edges of cells stopped at the end of the paths (180  $\mu\text{m}$ ). The time profiles were divided into two categories: red lines, for the cells whose protrusions extended beyond 120  $\mu\text{m}$  within 20 h; and blue lines, for the cells whose protrusions did not reach that point.

adhered to the paths as well as the array spots when both regions were illuminated simultaneously (Figure 2d). In addition, a nontoxic manner of activating substrate surface during cell cultivation is indispensable to the spatiotemporally controlled induction of cell protrusion.

To investigate the actin cytoskeleton and changes in subcellular structures of the two cell protrusions, cells were fixed at 6 h after induction of cell migration and subjected to immunofluorescence staining (Figure 3). On the wide path, actin stress fibers having vinculin-containing focal adhesions at both ends were formed in various angles (Figure 3a). On the narrow path, however, they were confined in parallel to the path with almost no variations in their angles (Figure 3b). The difference in the angles of actin filaments should affect cell motility because their dynamic assembling is the essential driving force for the cells' forward motion. Furthermore, the nuclei moved forward (left in Figure 3) outside the initial square spot probably because of cytosolic flow. These observations indicate that the further extension of cell protrusions results in directed cell migration over the illuminated paths.

To study the cell migration behavior of the two characteristic protrusions, we collected ample time profiles of the cells along wide and narrow paths. It is noteworthy that we were able to image the migration of single cells simultaneously using patterned illumination technology (Figure 4a).<sup>15</sup> The cells were found to migrate with various delay times, but the time profile slopes did not differ from one path to another within the same path width (Figure 4b and c). On the basis of this observation, we calculated the cell migration rates by measuring the lap time between one-third (60  $\mu\text{m}$ ) and two-thirds (120  $\mu\text{m}$ ) of the paths. The cells that did not reach the two-thirds point within 20 h were omitted from this calculation (Figure 4b and c, blue lines). The average migration rates along

the wide paths and the narrow paths were determined to be  $26.3 \pm 2.2$  and  $19.4 \pm 1.4$   $\mu\text{m}/\text{h}$ , respectively. Cell migration was statistically more rapid along the wide path than along the narrow path ( $P < 0.0005$ ). The slower migration rate along the narrow path was attributed to obstruction of cytoskeletal elongation in the restricted space (Figure 3b). Such quantitative analysis of the migration rates of single cells has been difficult to carry out, principally because the cells must be cultivated under identical conditions including cell shape and orientation and the number of contacting cells. Our photoactivatable substrate enabled parallel and flexible manipulation of single cells; this feature is important for dynamic single-cell analysis for quantitative biology.<sup>11</sup> Thus, the present method could be used for quantitative evaluation of the neurite elongation rate in response to various biochemical cues,<sup>7</sup> as one example.

In summary, we have developed a method for spatiotemporal control of the migration of single cells using a photoactivatable cell-culturing substrate. Selective formation of protrusions led by lamellipodia or filopodia and simultaneous measurement of the migration rates of single cells were achieved. Since the present method was successful under a conventional fluorescence microscope without additional instruments, it should be easily combined with advanced fluorescence imaging technologies to elucidate dynamic biochemical processes during cell migration.

**Acknowledgment.** This work was supported by a grant of Ecomolecular Science Research provided by RIKEN (to T.T and M.M.) and by the High-Tech Research Center Project from the Ministry of Education, Culture, Sports, Science, and Technology of Japan (to K.Y.). J.N. thanks the Special Postdoctoral Researcher Program of RIKEN.

**Supporting Information Available:** Experimental details are available. This material is available free of charge via the Internet at <http://pubs.acs.org>.

## References

- (1) Ridley, A.; Peckham, M.; Clark, P. *Cell Motility: From Molecules to Organisms*; Wiley: Chichester, UK, 2004.
- (2) Lauffenburger, D. A.; Horwitz, A. F. *Cell* **1996**, *84*, 359–369.
- (3) Yousaf, M. N.; Houseman, B. T.; Mrksich, M. *Proc. Natl. Acad. Sci. U.S.A.* **2001**, *98*, 5992–5996.
- (4) Yousaf, M. N.; Houseman, B. T.; Mrksich, M. *Angew. Chem., Int. Ed.* **2001**, *40*, 1093–1096.
- (5) Yeo, W. S.; Yousaf, M. N.; Mrksich, M. *J. Am. Chem. Soc.* **2003**, *125*, 14994–14995.
- (6) Kaji, H.; Kawashima, T.; Nishizawa, M. *Langmuir* **2006**, *22*, 10784–10787.
- (7) Dertinger, S. K. W.; Jiang, X. Y.; Li, Z. Y.; Murthy, V. N.; Whitesides, G. M. *Proc. Natl. Acad. Sci. U.S.A.* **2002**, *99*, 12542–12547.
- (8) Jeon, N. L.; Baskaran, H.; Dertinger, S. K. W.; Whitesides, G. M.; Van de Water, L.; Toner, M. *Nat. Biotechnol.* **2002**, *20*, 826–830.
- (9) Gunawan, R. C.; Silvestre, J.; Gaskins, H. R.; Kenis, P. J. A.; Leckband, D. E. *Langmuir* **2006**, *22*, 4250–4258.
- (10) Kumar, G.; Meng, J. J.; Ip, W.; Co, C. C.; Ho, C. C. *Langmuir* **2005**, *21*, 9267–9273.
- (11) Di Carlo, D.; Lee, L. P. *Anal. Chem.* **2006**, *78*, 7918–7925.
- (12) Parker, K. K.; Brock, A. L.; Brangwynne, C.; Mannix, R. J.; Wang, N.; Ostuni, E.; Geisse, N. A.; Adams, J. C.; Whitesides, G. M.; Ingber, D. E. *FASEB J.* **2002**, *16*, 1195–1204.
- (13) Brock, A.; Chang, E.; Ho, C. C.; LeDuc, P.; Jiang, X. Y.; Whitesides, G. M.; Ingber, D. E. *Langmuir* **2003**, *19*, 1611–1617.
- (14) Jiang, X. Y.; Bruzewicz, D. A.; Wong, A. P.; Piel, M.; Whitesides, G. M. *Proc. Natl. Acad. Sci. U.S.A.* **2005**, *102*, 975–978.
- (15) Nakanishi, J.; Kikuchi, Y.; Takarada, T.; Nakayama, H.; Yamaguchi, K.; Maeda, M. *J. Am. Chem. Soc.* **2004**, *126*, 16314–16315.
- (16) Nakanishi, J.; Kikuchi, Y.; Takarada, T.; Nakayama, H.; Yamaguchi, K.; Maeda, M. *Anal. Chim. Acta* **2006**, *578*, 100–104.
- (17) Liu, V. A.; Jastromb, W. E.; Bhatia, S. N. *J. Biomed. Mater. Res.* **2002**, *60*, 126–134.
- (18) Small, J. V.; Stradal, T.; Vignal, E.; Rottner, K. *Trends Cell Biol.* **2002**, *12*, 112–120.
- (19) Wood, W.; Martin, P. *Int. J. Biochem. Cell Biol.* **2002**, *34*, 726–730.

JA070294P